

Advanced Oil Sorbents using Sequential Infiltration Synthesis

Edward Barry¹, Anil U. Mane², Joseph A. Libera², Jeffrey W. Elam², and Seth B. Darling^{1,3,*}

¹ Center for Nanoscale Materials, Argonne National Laboratory,
9700 South Cass Avenue, Lemont, Illinois 60439, USA.

² Energy Systems Division, Argonne National Laboratory,
9700 South Cass Avenue, Lemont, Illinois 60439, USA.

³ Institute for Molecular Engineering, University of Chicago,
5801 South Ellis Avenue, Chicago, Illinois 60637, USA.

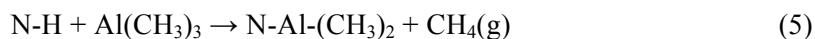
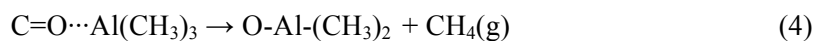
* Corresponding Author: darling@anl.gov, (630) 252-4580

Supplementary Information

FTIR data analysis

In the first region of Figure 2 in the main text, and Figures **Supplementary Figure S1-2**, major peaks observed were assigned according to^{1,2}. The sharp peak at $\sim 687\text{ cm}^{-1}$ corresponds to the methyl rocking mode for Al-CH₃ species indicating adsorbed TMA, but not revealing whether the TMA is physisorbed (intact) or chemisorbed (Al-CH₃ bonds are broken). In the second region, reduction of the carbonyl vibrational feature at $\sim 1725\text{ cm}^{-1}$ and 1640 cm^{-1} indicate complexation of the TMA molecules with these moieties. The third feature at $\sim 3300\text{ cm}^{-1}$ indicates that the N-H species present on the polyurethane backbone also participate in binding of the TMA molecules. Importantly, these raw spectra suggest nearly complete consumption of the C=O and N-H species in the polyurethane foam. Additional details can be observed by examining the FTIR difference spectrum between the TMA dosed foam and the bare PU foam (Fig. 2c). In the difference spectrum, positive features indicate the creation of new species whereas negative features signal the consumption of species. In addition to the peaks mentioned above, we observe a peak at 2923 cm^{-1} , associated with the C-H stretches for TMA methyl groups, as well as increases at 1575 cm^{-1} and 1188 cm^{-1} , and a decrease at 1100 cm^{-1} . We attribute the increase at 1575 cm^{-1} to a red-shift in the C=O stretching frequency caused by physisorption of TMA to C=O in analogy with our

previous study of TMA interaction with PMMA^{3,4}. Moreover, the decrease at 1100 cm⁻¹ and increase at 1188 cm⁻¹ are caused by physisorption of TMA to C-O-C species and the concurrent blue shift associated with a resonance effect between the C=O and C-O-R surface groups^{3,4}. We monitored these spectral changes versus time for 60 minutes after the TMA dose (see **Supplementary Figure S1**) and found that the changes in the C=O and C-O-R features reversed by ~20% over this time period, as did the Al-CH₃ rock at 686 cm⁻¹ and the C-H stretches for TMA at 2923 cm⁻¹. At the same time, absorption increased in the 750-950 cm⁻¹ region, which we attribute to Al-O modes. However, the N-H absorption at 3150-3400 cm⁻¹ did not change over the 60 minutes. We summarize these results from the reaction between polyurethane and TMA as follows:



In reaction (3), TMA reacts with the C=O groups of the polyurethane to form a physisorbed complex. This reaction is fast, and an equilibrium concentration of the physisorbed complex is rapidly achieved in under 180 seconds. In reaction (4), the physisorbed TMA reacts to form a permanent O-Al covalent linkage. Reaction (5) is the irreversible reaction between TMA and N-H groups to form a permanent N-Al bond releasing methane gas. Importantly, the absolute magnitude of the spectral changes are large, indicating that a substantial fraction of the available C=O and N-H functional groups have been consumed (see **Supplementary Figure S2 – Absolute FTIR Difference Spectra**). Reactions 4 and 5 each release one methyl ligand from TMA, and this is consistent with the low initial value of $x = 0.85$ observed by in situ mass spectrometry in Figure 1b, bottom. The fact that our measurements yield $x < 1$ in the early ALD Al₂O₃ cycles on the PU

foam suggests that some of the TMA remains intact (Eq. 3) so that all of the methyls are lost during the subsequent H₂O exposure.

Mass change data analysis

This experiment was repeated over a range of TMA exposure times (0.5-120 seconds) keeping all other parameters fixed. Under a single cycle, we expect an Al₂O₃ thickness of ~0.15 nm, independent of exposure time. Figure 1d shows the Al₂O₃ thicknesses measured at exposure times of 5 and 30 seconds. At low exposures (< 5 s), the thicknesses were roughly constant at 0.18 ± 0.07 nm. At longer exposures, however, the Al₂O₃ thicknesses were much larger and depended strongly on the position of the silicon witness piece relative to the foam. In particular, Al₂O₃ thickness was highest directly downstream of the foam and then decreased with distance further downstream. In addition, the thicknesses were an order of magnitude larger than expected. In contrast, witness pieces placed upstream of the first foam cube yielded thicknesses of ~0.2 nm regardless of exposure time. Ellipsometric fitting of the anomalously thick films yielded low refractive index values of ~1.4 consistent with organic material incorporated in the Al₂O₃. Little to no dependency on N₂ purge time (up to 400 s) and H₂O exposure time (up to 1200 s) was observed. The simplest explanation for these observations is that organic material is expelled by the foam during the TMA exposures (presumably from exothermic heating), which then settles onto the downstream Si surfaces. In a series of additional experiments, we compared conditions for which the integrated exposure time (number of cycles × exposure time) was varied. Five growth cycles at 15 s exposure produced non-uniform and anomalously large thicknesses (up to 30 nm), while five growth cycles at 1 s second exposures produced uniform thicknesses on the order of 5 nm (see **Supplementary Figure S4-5**). Similarly, changes in the foam mass were found to increase monotonically with TMA exposure time (see **Supplementary Figure S6**), providing a complimentary approach to investigating the nature of the SIS functionalization as

described in more detail below. These observations unequivocally demonstrate that the primary control parameter (for a given partial pressure) is the TMA chemical dosage or exposure time.

Thermodynamics of SIS reactions with foam

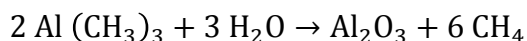
At a relatively modest TMA exposure time of 240 seconds, we observed a significant and irreversible expansion of the foam (see **Supplementary Figure S7**), followed by a violent explosion and complete disintegration when exposed to water. We associated these observations with the exothermic nature of the TMA to Al_2O_3 conversion coupled with the high specific surface area and low thermal conductivity of the foam. Thermodynamic calculations (HSC Chemistry 6.1, Outokumpu Research Oy, Pori, Finland, 2001) show that the reaction enthalpy for TMA and H_2O to form Al_2O_3 and CH_4 is $\Delta H = -146$ kcal / metal atom at 50 °C (see **Supplementary Table 1**). Assuming a stoichiometry of $\text{C}_{1.00}\text{H}_{1.75}\text{O}_{0.31}\text{N}_{0.07}$ and a heat capacity of 2.5 J/(g K) for the foam⁵, and further assuming that the enthalpy is released equally during both of the SIS half-reactions, then the complete consumption of N-H and C=O functional groups would produce a temperature rise of ~2000 K if all of this heat remains in the foam. While there is no doubt heat lost to the carrier gas and reactor walls, it is easy to see how the porous foam could achieve thermal runaway where the diffusion and reaction rates increase exponentially during the precursor exposures. Further evidence for this phenomenon was obtained by running the SIS reaction at different temperatures; the foam mass gain increased substantially over the range 60–110 °C (see **Supplementary Figure S8**).

Limiting precursor exposure

The saturation mass gain with TMA exposure time can be compared to estimates for the lower and upper limit mass gains. A lower limit assumes that only the outer surface of the 10 m²/g foam becomes coated with Al_2O_3 of thickness 0.15 nm and density of 2.9 g/cm³ (the ALD growth per cycle and density, respectively at 50 °C⁶). This estimate yields a lower limit of ~0.4% per cycle.

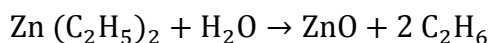
Similarly, an upper limit mass gain assumes complete infiltration of the polymer bulk such that all of the C=O and N-H groups react to form Al(OH)₂* (reactions 2, 4, 5). Assuming a stoichiometry of C_{1.00}H_{1.75}O_{0.31}N_{0.07}, this would produce a 118% mass gain. The plateau at ~5% in Figure 3 is intermediate between the lower and upper limit mass gains suggesting a small, relatively constant infiltration of the Al₂O₃ SIS into the near surface region of the PU foam. Assuming that the TMA diffuses radially from the surface of circular PU ligaments of radius ~50 μm (see Figure 1a), the 5% mass gain indicates ~1 μm infiltration. This value will depend upon the relative rates for TMA diffusion through the macro- and micro-pores of the polymer as well as the reaction rate of TMA with PU, all of which are temperature-dependent.

Supplementary Table 2.
TMA/H₂O calculation.



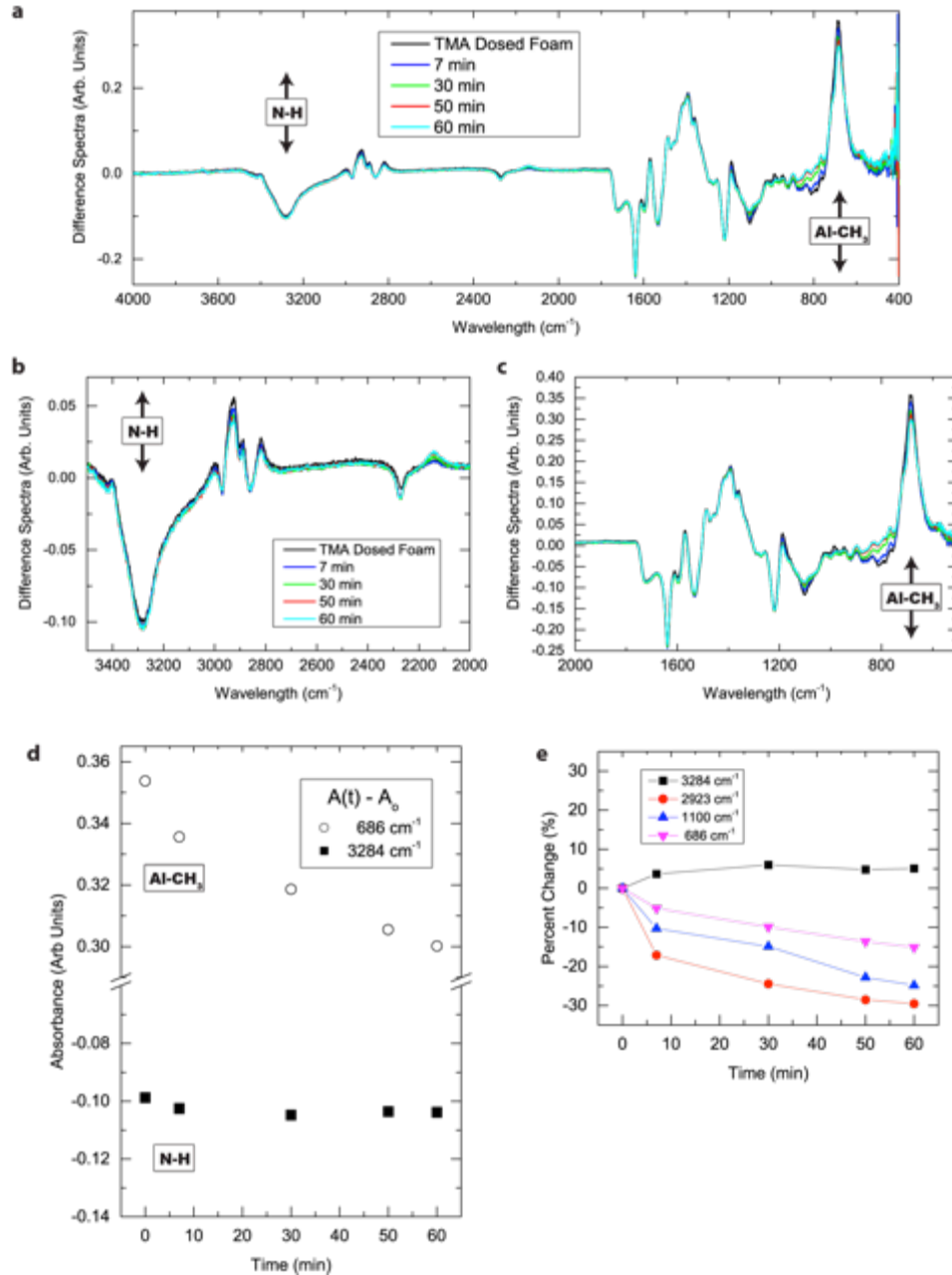
Temperature	ΔH	ΔS	ΔG	ΔH/metal atom
°C	kcal/mol	cal/K mol	kcal/mol	kcal/mol
0.000	-292.914	-24.360	-286.260	-146.457
50.000	-292.552	-23.146	-285.073	-146.276
100.000	-292.116	-21.895	-283.946	-146.058
200.000	-290.845	-18.905	-281.900	-145.423
300.000	-288.960	-15.309	-280.185	-144.480
400.000	-286.488	-11.345	-278.851	-143.244
500.000	-283.516	-7.237	-277.921	-141.758
600.000	-280.092	-3.077	-277.405	-140.046
700.000	-276.219	1.118	-277.307	-138.110
800.000	-271.948	5.293	-277.627	-135.974
900.000	-267.317	9.416	-278.363	-133.659
1000.000	-262.370	13.461	-279.508	-131.185

Supplementary Table 3.
DEZ/H₂O calculation.



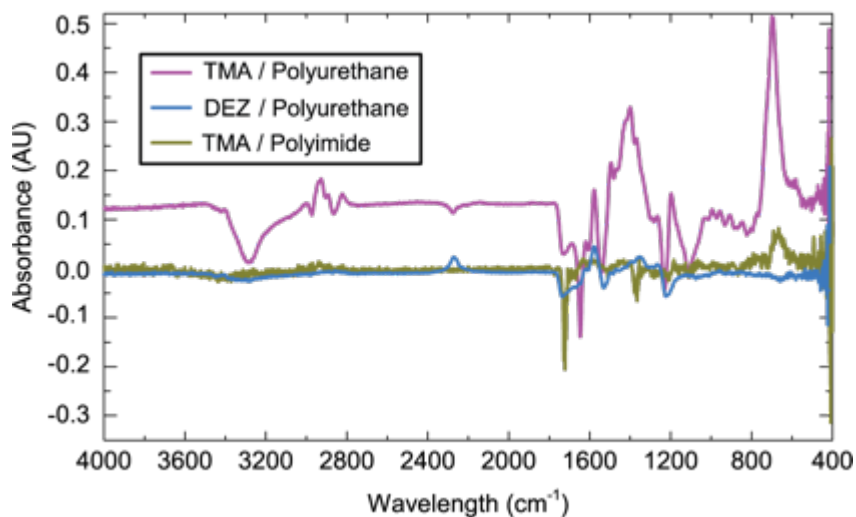
Temperature	ΔH	ΔS	ΔG	$\Delta H/\text{metal atom}$
$^{\circ}\text{C}$	kcal/mol	cal/K mol	kcal/mol	kcal/mol
0.000	-70.011	9.761	-72.677	-70.011
50.000	-70.536	7.995	-73.119	-70.536
100.000	-71.008	6.635	-73.484	-71.008
200.000	-71.651	5.085	-74.057	-71.651
300.000	-71.655	5.052	-74.551	-71.655
400.000	-70.730	6.518	-75.117	-70.730
500.000	-68.578	9.475	-75.904	-68.578
600.000	-64.901	13.928	-77.062	-64.901
700.000	-59.391	19.883	-78.740	-59.391
800.000	-51.730	27.358	-81.089	-51.730
900.000	-59.726	6.222	-67.025	-59.726
1000.000	-69.077	-1.421	-67.267	-69.077

SUPPLEMENTARY FIGURES

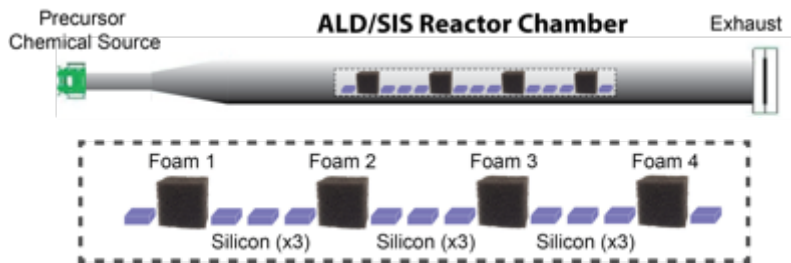


Supplementary Figure S1 – FTIR Time Behavior - a. FTIR difference spectra, comparing the difference between trimethylaluminum (TMA) dosed polyurethane foam and the bare foam, is plotted as a function of wait time after the TMA exposure. Difference spectra are shown for the foam after TMA exposure, and after wait times of 7 minutes (red), 30 minutes (green), 50 minutes (blue), and 60 minutes (cyan). **b.** and **c.** Identical data plotted over smaller wavelength range. **d.** The difference in absorbance is plotted as a function of wait time for two different vibrational frequencies, 686 cm^{-1} (open circles) and 3284 cm^{-1} (black solid squares). Here, the

absorbance difference was defined as the difference between the absorption at time t minus the initial absorbance at time $t=0$, $A_x(t) - A_x(0)$, where $x = 685 \text{ cm}^{-1}$ and $x = 3284 \text{ cm}^{-1}$. The vibrational frequency of 686 cm^{-1} corresponds to Al-CH₃ groups and 3284 cm^{-1} to N-H groups. **e.** Equivalent percent change of the absorbance data shown in **d.** is shown for all peak locations described in the text.

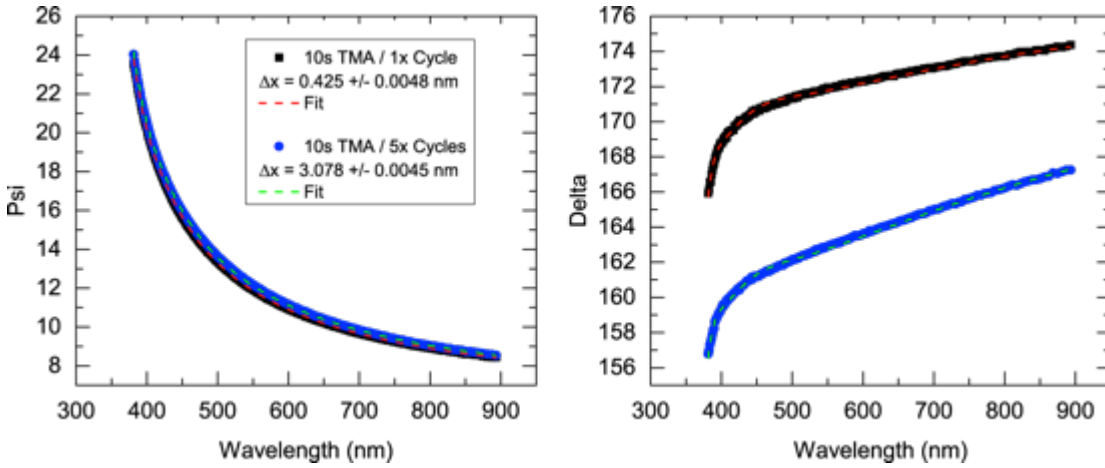


Supplementary Figure S2 – FTIR Difference Spectra - FTIR difference spectra, comparing the difference between the precursor dosed foam and the bare foam, is shown for TMA/polyurethane (purple), DEZ/polyurethane (blue), and TMA/polyimide (yellow). In comparison with the data shown in Fig.2 of the main text, difference spectra shown here have not been rescaled, and represent the actual difference.

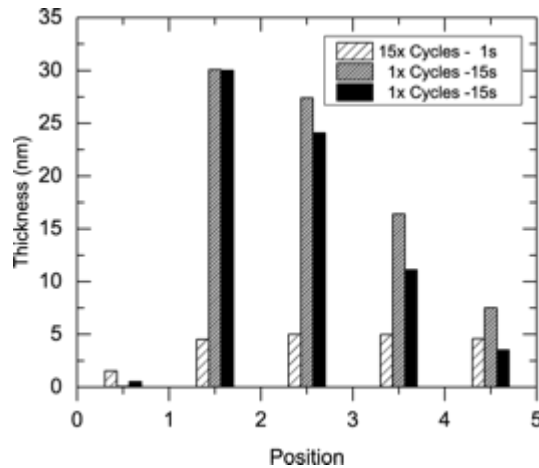


Supplementary Figure S3 - Schematic of the SIS reactor geometry and experimental setup. Schematic of the distant-dependent reactor setup, similar to that shown in Fig 1e in the main text and reproduced here for interpreting the Supplementary Figures below. Chemical vapor flow proceeds from left (precursor chemical source) to right (exhaust). Magnified view of the tray as

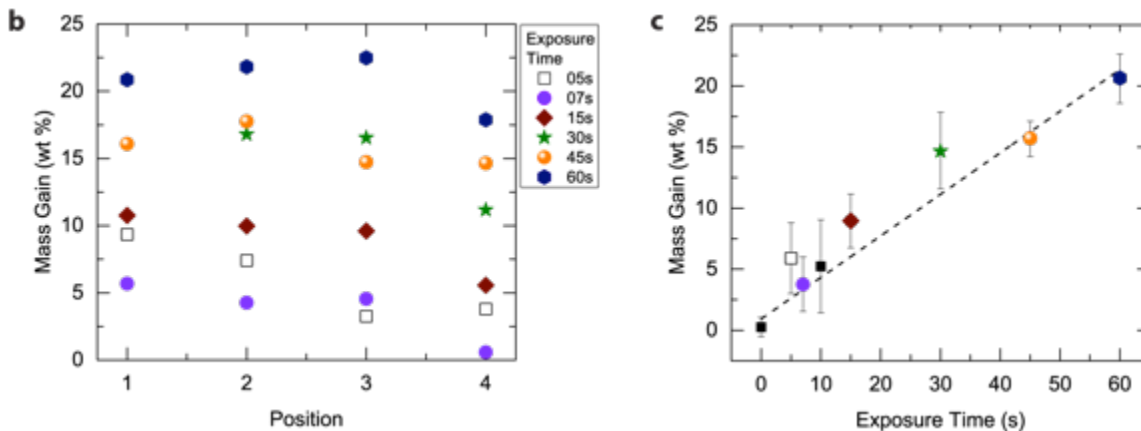
loaded into the reactor chamber, containing four (4×) pieces of foam. Silicon witness pieces were placed in between the foam, and at the beginning and ends of the reactor. Each piece of foam is separated by an actual distance of 3.5”.



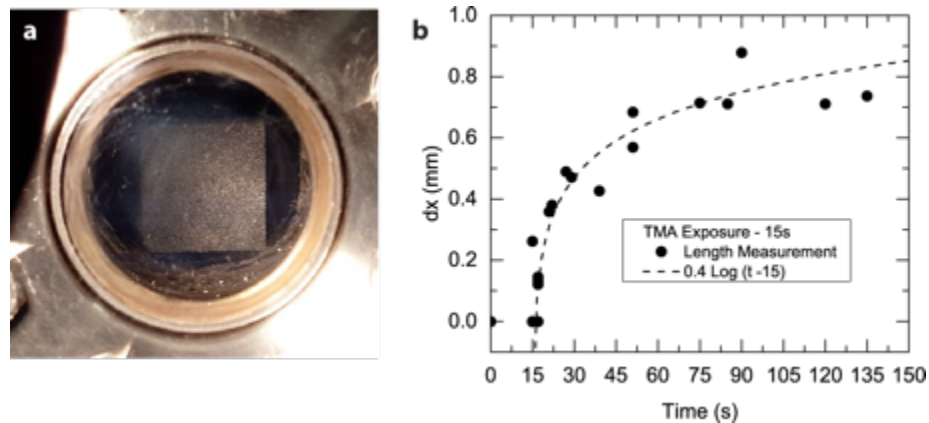
Supplementary Figure S4 – Ellipsometry Fitting. Two examples of ellipsometry fitting on silicon witness for identical TMA exposures of 10 seconds (80 °C, 0.4 torr) using 1× TMA/H₂O cycle (black) and 5× TMA/H₂O cycles (blue). Data are shown for the silicon witness piece directly after the first piece of foam. Fits are overlaid onto the data using red and green dashed lines for the 1× and 5× cycles respectively. Fits were performed using a Cauchy model for the aluminum oxide layer, from which deposited thicknesses of 0.425 nm and 3.078 nm were measured for the 1× and 5× cycles, respectively.



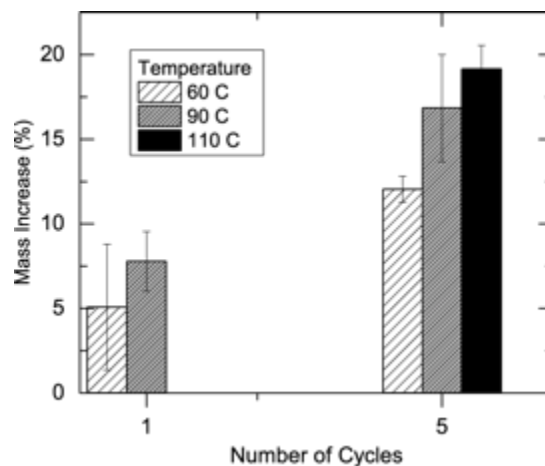
Supplementary Figure S5 – Integrated Exposure Time Thickness obtained via ellipsometry on silicon witness pieces used to illustrate the effect of integrated exposure time. Data are shown for $15\times$ cycles of a 1 second TMA exposure (white bar graphs) and $5\times$ cycles of 15 second TMA exposure (grey bar graphs). Temperature and pressure remained fixed in both cases at 80 °C and 0.4 Torr. Data are plotted as a function of the silicon witness piece position inside the reactor. Single Si witness pieces were placed at equally spaced intervals between the 4 pieces of foam, located at positions $x = 1.5, 2.5, 3.5,$ and 4.5 . The first set of thickness data, positioned at $x = 0.5$, was recorded on a witness piece placed *before* the first piece of foam (positioned at $x = 1$), closest to the chemical source. The effects of long TMA exposure and small cycle number versus a short TMA exposure and large cycle number are clearly evident: the 15 second exposure results in a measured thickness of ~ 30 nm after $5\times$ cycles, while $5\times$ cycles at 1 second exposure result in ~ 5 nm. In typical ALD, one would expect the $15\times - 1$ s exposure sequence to produce a uniformly larger thickness than the $5\times - 15$ s sequence. Solid black bar graphs correspond to a 1200 second water exposure with identical TMA exposure / cycle number conditions as that shown in gray, $5\times$ cycles of 15 second TMA exposure. Despite the roughly two order of magnitude difference, little to no change is observed in the deposited thickness.



Supplementary Figure S6 – TMA Foam Mass **a.** Masses of the foam before and after SIS treatment is plotted as a function of position inside the reactor for various TMA exposure times over a range of 5-60 seconds. Data are shown for polyurethane foams under $1\times$ cycle of aluminum oxide growth as a function of spatial location inside the reactor, with position 1 located closest to the chemical source. Different colors correspond to different TMA exposure times as shown in the legend. Weight percentage was calculated using the ratio of foam mass before and after SIS treatment. The average initial foam mass was ~ 372 mg. **b.** Averaging over the four pieces of foam at a given exposure time, the average mass gain (in weight percentage) is plotted as a function of exposure time. Error bars represent standard deviations in the measurements. Two additional points at exposure times of 10 seconds, and 0 seconds are shown in black squares, with the latter serving as a baseline measurement to investigate the influence of N_2 purges, H_2O exposure, and the temperature effects of the reactor ($80^\circ C$). The negligible mass increase confirms that these effects did not contribute to the mass gain. Data over the entire exposure range were fit using a line with a slope of 0.34 and an intercept of 0.9 (dashed black line). The line approximates the data reasonably well at the high exposure limit (>10 s) where the mass gain is monotonically increasing with exposure time. These identical data are plotted on a linear-log scale in Figure 3 of the paper.

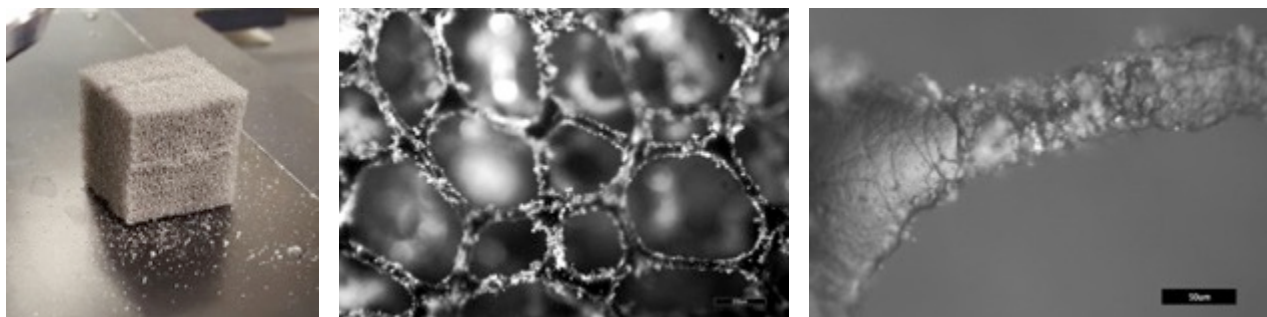


Supplementary Figure S7 – Foam Expansion – **a.** Still image extracted from Supplementary Movie S1, measuring the change in foam volume upon exposure to TMA. **b.** The change in distance between two defects on the foam, measured via image analysis (ImageJ) was used to quantify a linear expansion of the foam upon exposure to TMA. As shown, TMA exposure begins at time $t = 15$ s, at which point the foam quickly expands, reaching a type of saturation in ~ 40 seconds. The corresponding change in length between the two foam defects, dx was reasonably well approximated by a logarithmic fit, $dx \sim 0.4 \text{ Log}(t-15)$, shown by the dashed line.

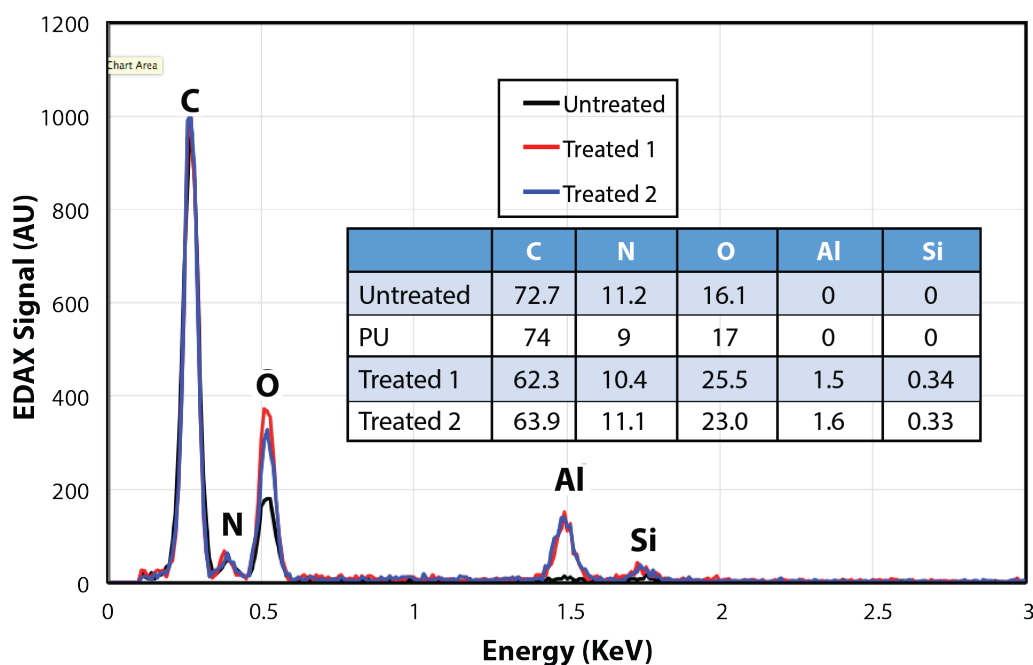


Supplementary Figure S8 – Foam Mass Gain vs. Temperature - Foam mass gain is plotted in terms of weight percentage for (i) $1\times$ and (ii) $5\times$ aluminum oxide growth cycles at a TMA exposure of 10 seconds, 0.4 Torr. Different bar graphs correspond to different temperatures as described in the legend. At higher temperatures, the mass gain increases accordingly. Data

represent the average mass gain, averaged over 4 identical foams loaded into the reactor (see Supplementary Figure S1). Error bars represent standard deviations to the averages.

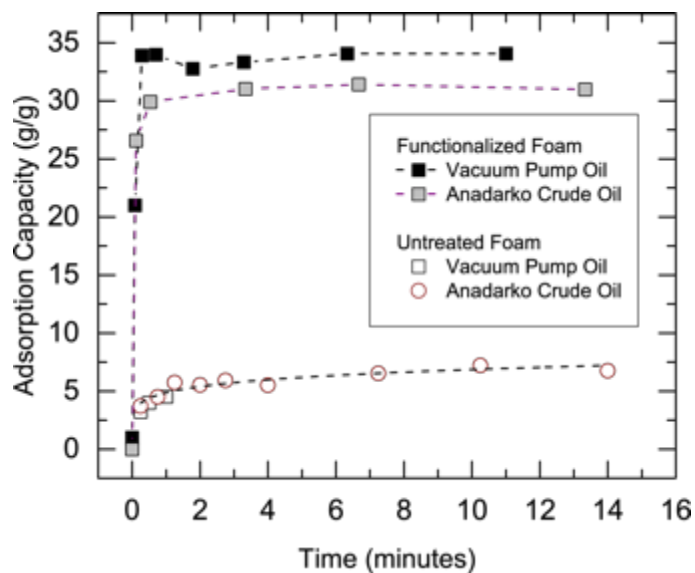


Supplementary Figure S9 - Polyurethane Compression Cycles - Photograph and optical micrographs of an over-exposed SIS-treated foam following repeated compression cycles. Foam was functionalized using 10× cycles of aluminum oxide growth at 10 second TMA exposure, 80 °C, and 0.4 Torr. Images show visible changes in fiber structure.

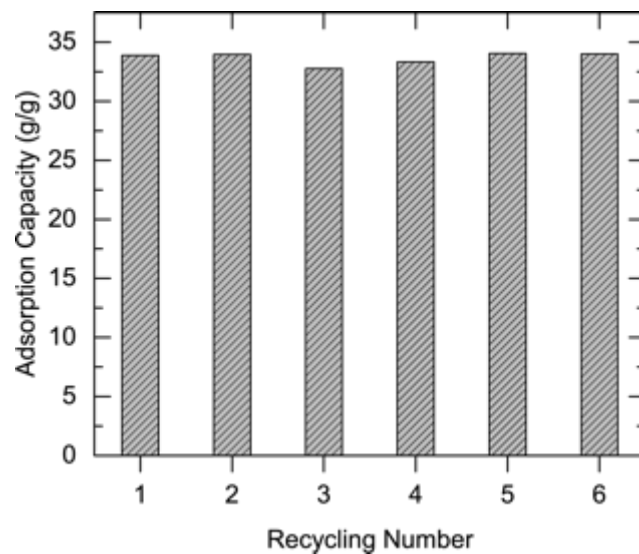


Supplementary Figure S10 – EDAX Analysis – Energy dispersive X-ray spectroscopy analysis of untreated (black solid line) and SIS/silane - treated polyurethane (PU) foam. Two sets of data were recorded for the SIS-treated piece of foam located in different locations on the same sample (blue and red lines). Foam was functionalized using 1× cycle of aluminum oxide growth at 5 s TMA exposure, 80 °C, and 0.4 torr. Chemical elements are listed at their respective energies for carbon, nitrogen, oxygen, aluminum, and silicon. (inset) Table listing the measured values (in terms of percentage of EDAX signal) for the untreated foam (first row), and two locations on the treated foam (third and fourth rows). The second row contains calculated values for polyurethane

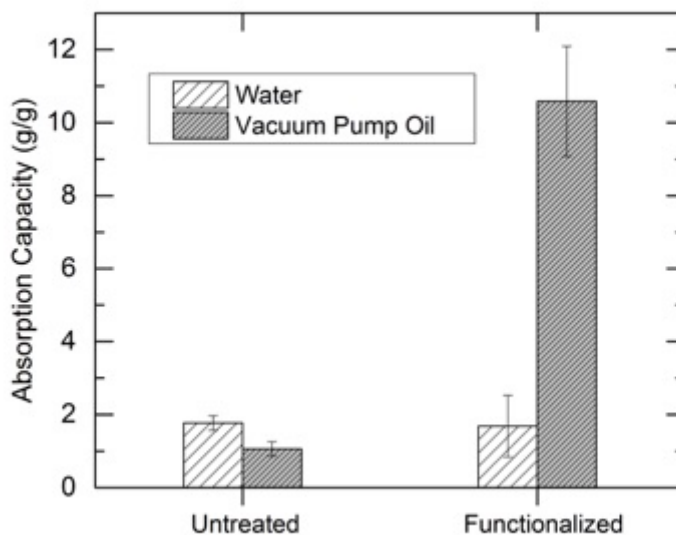
based upon its chemical structure. In comparison with the first row, recorded EDAX signals for the untreated foam are very close to expected values for polyurethane, while characteristic Al and Si signals in the case of the treated confirm SIS/silane functionalization.



Supplementary Figure S11 – Sorption Kinetics Sorption of hydrocarbon-based vacuum pump oil and crude oil (Anadarko) plotted as a function time for untreated and SIS/silane functionalized polyurethane foam.

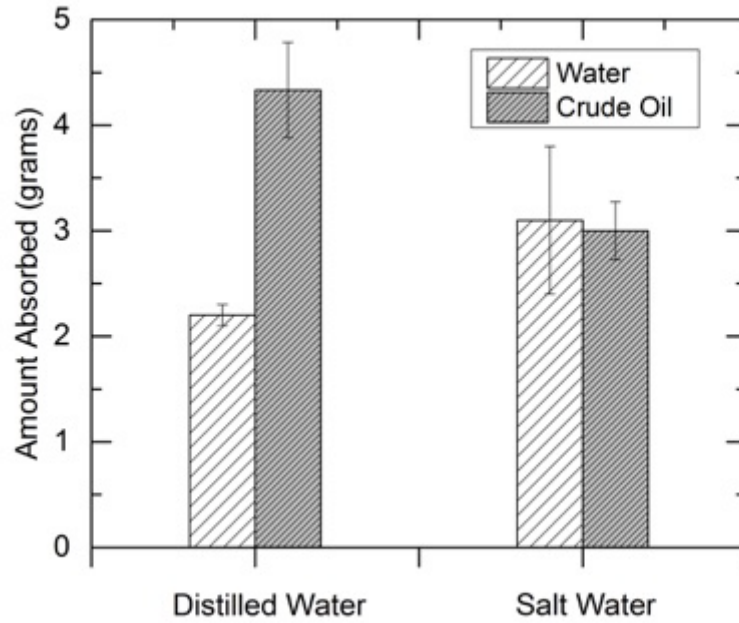


Supplementary Figure S12 – Recycling Number/Reusability - Oil sorption capacity of vacuum pump oil following multiple cycles of compression and re-sorption, demonstrating reusability properties of SIS/silane treated foams. Data were obtained following reusability tests outlined in Section 10 of the ASTM Standard: Test Method for Sorbent Performance of Adsorbents, F726.



Supplementary Figure S13 – Oil/Water Selectivity – Maximum Sorption Capacities. Foam sorption selectivity with respect to oil and water was quantified using the maximum sorption tests as described in the text (see also Section 9 of the ASTM Standard F726). Briefly, foams were immersed in a particular solvent for 15 minutes, removed, and allowed to drain for 30 seconds.

The weight of the foam before and after immersion was then compared. Data are shown for untreated and SIS-treated / oleophilic functionalized foams.



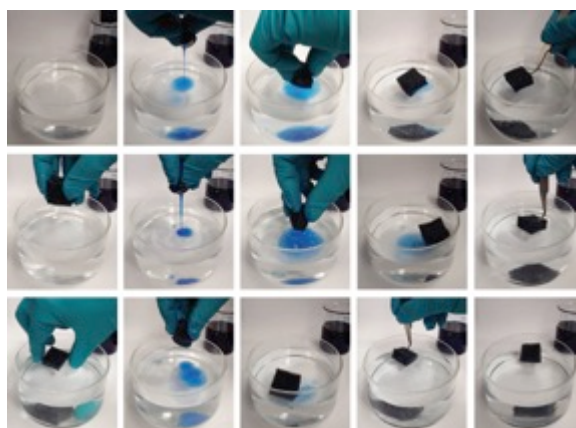
Supplementary Figure S14 – *Salt Water Tests*. Comparison of sorption tests for distilled water and model sea water.

SUPPLEMENTARY MOVIES

Supplementary Movie 1 – *TMA Explosion Video*

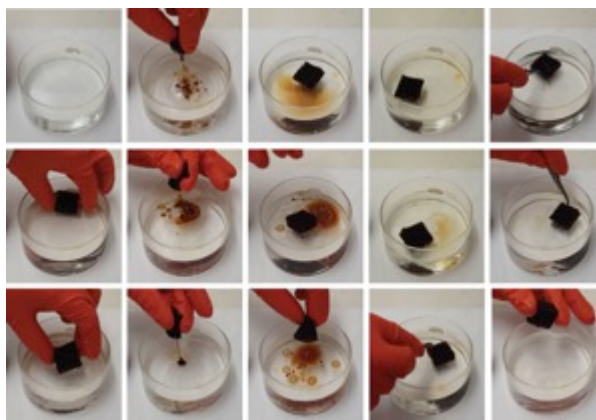


Supplementary Movie 2 – *Silicone Oil Sorption*



Oil sorption tests carried out with dyed silicone oil on the surface of water. Still images extracted from Supplementary Movie 2.

Supplementary Movie 3 – *Crude Oil Sorption*



Oil sorption tests carried out with crude oil on the surface of water. Still images from Supplementary Movie 3.

Supplementary References

1. Radice, S., Turri, S. & Scicchitano, M. Fourier transform infrared studies on deblocking and crosslinking mechanisms of some fluorine containing monocomponent polyurethanes. *Applied Spectroscopy* **58**, 535-542 (2004).
2. Gong, B. & Parsons, G.N. Quantitative in situ infrared analysis of reactions between trimethylaluminum and polymers during Al₂O₃ atomic layer deposition. *Journal of Materials Chemistry* **22**, 15672-15682 (2012).
3. Biswas, M., Libera, J.A., Darling, S.B. & Elam, J.W. New Insight into the Mechanism of Sequential Infiltration Synthesis from Infrared Spectroscopy. *Chemistry of Materials* **26**, 6135-6141 (2014).
4. Biswas, M., Libera, J.A., Darling, S.B. & Elam, J.W. Kinetics for the Sequential Infiltration Synthesis of Alumina in Poly(methyl methacrylate): An Infrared Spectroscopic Study. *Journal of Physical Chemistry C* **119**, 14585-14592 (2015).
5. Pau, D.S.W., Fleischmann, C.M., Spearpoint, M.J. & Li, K.Y. Thermophysical properties of polyurethane foams and their melts. *Fire and Materials* **38**, 433-450 (2014).
6. Groner, M.D., Fabreguette, F.H., Elam, J.W. & George, S.M. Low-temperature Al₂O₃ atomic layer deposition. *Chemistry of Materials* **16**, 639-645 (2004).